INFECTION AND IMMUNITY, June 2003, p. 3419–3428 Vol. 71, No. 6
0019-9567/03/$08.00+0 DOI: 10.1128/IAI.71.6.3419–3428.2003

Antigenic Composition of *Borrelia burgdorferi* during Infection of SCID Mice

Timothy R. Crother,[1,2]* Cheryl I. Champion,[1,2] Xiao-Yang Wu,[1,2] David R. Blanco,[1,2] James N. Miller,[2] and Michael A. Lovett[1]

Departments of Medicine[1] and Microbiology, Immunology, and Molecular Genetics,[2] University of California, Los Angeles, Los Angeles, California

Received 6 November 2002/Returned for modification 16 December 2002/Accepted 7 March 2003

The general concept that during infection of mice the *Borrelia burgdorferi* surface protein composition differs profoundly from that of tick-borne or in vitro-cultivated spirochetes is well established. Specific knowledge concerning the differences is limited because the small numbers of spirochetes present in tissue have not been amenable to direct compositional analysis. In this report we describe novel means for studying the antigenic composition of host-adapted *Borrelia* (HAB). The detergent Triton X-114 was used to extract the detergent-phase HAB proteins from mouse ears, ankles, knees, and hearts. Immunoblot analysis revealed a profile distinct from that of in vitro-cultivated *Borrelia* (IVCB). OspA and OspB were not found in the tissues of SCID mice 17 days after infection. The amounts of antigenic variation protein VlsE and the relative amounts of its transcripts were markedly increased in ear, ankle, and knee tissues but not in heart tissue. VlsE existed as isoforms having both different unit sizes and discrete lower molecular masses. The hydrophobic smaller forms of VlsE were also found in IVCB. The amounts of the surface protein (OspC) and the decorin binding protein (DbpA) were increased in ear, ankle, knee, and heart tissues, as were the relative amounts of their transcripts. Along with these findings regarding VlsE, OspC, and DbpA, two-dimensional immunoblot analysis with immune sera also revealed additional details of the antigenic composition of HAB extracted from ear, heart, and joint tissues. A variety of novel antigens, including antigens with molecular masses of 65 and 30 kDa, were found to be upregulated in mouse tissues. Extraction of hydrophobic *B. burgdorferi* antigens from tissue provides a powerful tool for determining the antigenic composition of HAB.

Several key developmental events mark the transmission of *Borrelia burgdorferi* from feeding ticks to mammalian hosts. As ticks ingest a blood meal, synthesis of the surface protein OspA is downregulated as midgut spirochetes multiply and migrate to the salivary glands. In parallel, synthesis of another surface lipoprotein, OspC, is enhanced (13, 46). After transmission, OspA synthesis remains repressed (4, 12, 37). Antigenic variation of the surface lipoprotein VlsE is initiated (60) and is likely to be an important facet of *B. burgdorferi* virulence (29, 41). Recently, it has been shown that *ospC* synthesis wanes in apparent response to the synthesis of OspC antibody by infected mice (31). There has been growing appreciation that surface changes that distinguish host-adapted *Borrelia* (HAB) from tick-borne *B. burgdorferi* are likely to be related to protective immunity (47).

Much effort has therefore been directed at defining the structural differences between HAB and in vitro-cultivated *Borrelia* (IVCB). The small numbers of HAB found in the tissues of infected mice have been regarded as insufficient for direct protein and antigenic analysis. PCR-based methods have detected 3×10^5 spirochetes per mg of mouse ear DNA (2), as well as 10^6 spirochetes per mg of heart DNA and 3×10^5 spirochetes per mg of joint DNA in both C3H and C3H-SCID mice (2, 35, 57). Because mouse ears, hearts, and joints contain severalfold less than 1 mg of DNA (Champion, unpublished observations) and because there may be many copies of the chromosome in each spirochete (26, 47), the actual numbers of HAB in a mouse may be less than the numbers given above seem to indicate.

A variety of genetic approaches have therefore been employed to search for genes differentially expressed by HAB and IVCB. In two recent studies the researchers examined genes downregulated during infection in response to immune pressure (31, 34). Liang et al. showed that *ospC* is downregulated soon after infection of immunocompetent mice but not after infection of SCID mice (31). Liang and colleagues used reverse transcription PCR (RT-PCR) to determine whether 137 lipoprotein genes were expressed during skin infection of normal and SCID mice; 97 of these genes were downregulated in immunocompetent mice (34). The genes upregulated during infection include *eppA* (7), *pG* (55), *bbk2.1* (1), *ospE* paralogues (54), *p35* or the gene encoding fibronectin binding protein, *bbk32* (16, 40, 53), and *p37* (53), as well as *dbpA* (6, 21). However, because HAB strains have not been available for direct study, the full set of genes upregulated during infection, the quantitative extent of upregulation, and the cellular location of upregulated proteins have remained unknown or have been inferred. There has been only one study in which intact HAB strains were used for structural analysis of any sort. Using immunofluorescence, Montgomery and colleagues showed that OspC could be detected on the surface of *B. burgdorferi* recovered from mice by peritoneal washing (37). Pathogenic mechanisms that have been elucidated, such as

* Corresponding author. Mailing address: Department of Medicine, Division of Infectious Diseases, University of California, Los Angeles, 37-121 Center for Health Sciences, 10833 LeConte Ave., Los Angeles, CA 90095. Phone: (310) 825-4188. Fax: (310) 267-2265. E-mail: tcrother@ucla.edu.

VlsE antigenic variation, have been examined by using genetic strategies (58–60) rather than direct analysis of HAB.

In this report, we describe new methods that allow direct determination of the HAB protein composition in ear, joint, and heart tissues of immunodeficient mice. By extracting hydrophobic HAB proteins from tissues and then performing immunoblotting with two-dimensional gels, we were able to visualize the constellation of major changes that comprise the early stage of spirochetal adaptation to the host environment.

MATERIALS AND METHODS

Bacterial strains. Virulent *B. burgdorferi* sensu stricto strain B31 was isolated from infected rabbit skin and grown at 34°C in BSKII supplemented with 6% normal rabbit serum as described previously (17). Low-passage (≤3 passages) virulent B31 was used in all experiments. Strain ME3-2 is a B31 clonal isolate that was grown from SCID mouse blood and lacks *vlsE* (data not shown).

Infection of C3H SCID mice with *B. burgdorferi*. Seven-week-old C3HSmn .CB17-*Prkdc*^{scid}/*J* (C3H SCID) mice (Jackson Laboratory, Bar Harbor, Maine) were inoculated intradermally with 10^7 virulent *B. burgdorferi* B31 cells. Seventeen days later, the animals were sacrificed, and the ears, ankles, knees, and hearts were collected and snap frozen in an ethanol-dry ice bath.

RT-PCR. A DNeasy tissue kit from Qiagen (Valencia, Calif.) was used according to the manufacturer's instructions to obtain genomic DNA from tissue samples and IVCB. Purified DNA samples were ethanol precipitated and resuspended in 50 μl of water. Primers and probes were selected for the flagellin gene (GenBank accession no. AE001126) for use in quantitation of *B. burgdorferi* strain B31 in infected tissues. The upstream primer for *flaB* corresponds to the region from base 579 to base 602 (TGTTGCAAATCTTTTCTCTGGTGA) of the open reading frame. The downstream primer corresponds to the region from base 635 to base 656 (CCTTCCTGTTGAACACCCTCTT). The probe corresponds to the region from base 609 to base 631 (TCAAACTGCTCAGGCTGC ACCGG). The nidogen gene (exon 2) was selected for murine tissue quantitation (GenBank accession no. L17323). The upstream primer for *nidogen-1* corresponds to the region from base 86 to base 105 (CACCCAGCTTCGGCTCA GTA) of the open reading frame. The downstream primer corresponds to the region from base 133 to base 148 (TCCCCAGGCCATCGGT). The probe corresponds to the region from base 107 to base 131 (CGCCTTTCCTGGCTGAC TTGGACAC). The probes were labeled with 6-carboxyfluorescein at the 5′ end and with 6-carboxy-*N*,*N*,*N*′,*N*′-teramethylrhodamine at the 3′ end. The primers were purchased from Invitrogen (Carlsbad, Calif.), and the probes were purchased from Qiagen. TaqMan universal PCR master mixture (Applied Biosystems, Foster City, Calif.) was used for all reactions. Each reaction mixture (25 μl) contained each primer at a concentration of 900 nM and the probe at a concentration of 250 nM. Amplification and detection were performed with an ABI 7700 system by utilizing the following parameters: 50°C for 2 min and 95°C for 10 min, followed by 40 cycles of 95°C for 15 s and 60°C for 1 min. The fluorescence was monitored continuously. The data were analyzed, and the cycle threshold value was determined by using the ABI Sequence Detection System software, version 1.9. Flagellin and nidogen reactions were performed in separate wells. One hundred nanograms of DNA from infected tissue was used for most reactions; the exceptions were the reactions for the ear tissue, for which 10 ng was used. The amounts of B31 and mouse DNA were calculated based on standard curves for a 6-log dilution series for *B. burgdorferi* and a 4-log dilution series for mouse DNA (Novagen, Madison, Wis.). Values for the B31 standard curve were obtained in the presence of 100 ng of mouse DNA. The copy number of each sample was determined by plotting the cycle threshold value versus the log of the copy numbers included in each standard curve. All samples were examined in triplicate. No-template controls were included with every assay for each primer set.

RT-PCR analysis of *vlsE*, *ospC*, and *dbpA* in HAB and IVCB. In order to determine the relative amounts of VlsE, OspC, and DbpA in HAB and IVCB, RT-PCR was performed as described previously (47). In this study, the flagellin subunit gene *flaB* was used as a normalizing control for HAB and IVCB. The following primer sets were used for the PCR: *flaB* forward (5′ CTGGCAAGA TTAATGCTCAA 3′) and *flaB* reverse (5′ CAGGAGAATTAACTCCACCT 3′); OspC forward (5′ GAAAAAGAATACATTAAGTGC 3′) and OspC reverse (5′ CTTGTAAGCTCTTTAACTGAA 3′); DbpA forward (5′ TAACTAT ACTTGTTAACCTAC 3′) and DbpA reverse (5′ AGTTTCTTTGAGTTTAG TAGC 3′); and VlsE forward (5′ AGATGATAACTTATACTTTTCATTA TA AGGAGACG 3′) and VlsE reverse (5′ ACGGCAGTTCCAACAGAACCTGT ACTATCT 3′). The PCR conditions were as follows: 94°C for 10 min to activate the AmpliTaq Gold (Perkin-Elmer, Norwalk, Conn.), followed by 40 to 45 cycles of denaturation at 94°C for 1 min, annealing at 48°C for 1 min, and elongation at 72°C for 1 min.

Extraction of hydrophobic HAB antigens from B31-infected tissues. Infected tissue was homogenized in a PowerGen 125 tissue grinder (Fisher Scientific Co., Pittsburgh, Pa.) in 10 mM Tris (pH 8.0)–1 mM EDTA–1 mM phenylmethylsulfonyl fluoride (approximately 50 mg of tissue/ml). Triton X-114 was added to a final concentration of 3%, and the samples were incubated overnight at 4°C with gentle rocking. Insoluble material was pelleted by centrifugation for 30 min at 16,000 × *g* at 4°C. The cell-free lysate was then incubated at 37°C for 5 min, and this was followed by centrifugation at 3,400 × *g* for 15 min at room temperature in order to generate aqueous and detergent phases. The detergent phase was washed three times with 10 mM Tris–1 mM EDTA (pH 8.0). IVCB were washed three times with phosphate-buffered saline and resuspended in 10 mM Tris (pH 8.0)–1 mM EDTA–1 mM phenylmethylsulfonyl fluoride. Triton X-114 extraction and precipitation were performed as described above. For sodium dodecyl sulfate (SDS)-polyacrylamide gel electrophoresis (PAGE) analysis, detergent-phase samples were precipitated by mixing them with 3 volumes of −20°C acetone and incubated at −20°C for 2 h. The precipitate was pelleted by centrifugation for 30 min at 16,000 × *g* and 4°C. The pellet was air dried and resuspended in final sample buffer. For two-dimensional electrophoresis analysis, detergent-phase samples were precipitated by addition of three volumes of 10% trichloroacetic acid–20 mM dithiothreitol (DTT) in −20°C acetone and incubated at −20°C for 2 h. The precipitate was pelleted by centrifugation at 16,000 × *g* for 30 min at 4°C, and the pellet was washed once with −20°C acetone containing 20 mM DTT. The pellet was then air dried and resuspended in 7 M urea–2 M thiourea–1% amidosulfobetaine-14 (8, 36).

SDS-PAGE and immunoblot analysis. Protein samples were separated by SDS-PAGE (12% acrylamide) by using the Laemmli method (30). The proteins were transferred to polyvinylidene difluoride membranes and stained with amido black. The membranes were probed with either immune rabbit serum (IRS) (diluted 1:1,000), αOspC (diluted 1:1,000), αVlsE (diluted 1:2,000), αDbpA (diluted 1:2,000), αBmpA (diluted 1:10,000), αLA7 (diluted 1:10), or mouse serum (diluted 1:1,000), each diluted in phosphate-buffered saline containing 0.05% Tween 20 and in 5% nonfat dry milk. For OspC, LA7, and mouse serum from B31 chronically infected mice (CMS), horseradish-linked sheep anti-mouse secondary antibody (Amersham Biosciences) was used at a dilution of 1:2,500 as a secondary antibody. For all other analyses, horseradish-linked donkey ant-rabbit antibody (Amersham Biosciences) was used at a dilution of 1:2,500. Visualization was performed with the ECL Plus system from Amersham Pharmacia Biotech and an Alpha Innotech Fluorchem 8000 imager. Band densitometry was performed with the Fluorchem imaging software (version 2.0). The following individuals provided antisera: Steven Norris, University of Texas at Houston (αVlsE) (unpublished data); Steven Callister, Gundersen Lutheran Medical Center (αOspC) (44); Felipe Cabello, New York Medical College (αBmpA) (unpublished data); and Magnus Hook, Texas A&M University (αDbpA) (20). Anti-LA7 monoclonal serum was provided by the Institut für Immunologie, Heidelberg Germany (19, 56). IRS was obtained from rabbits with complete infection-derived immunity to reinfection (17, 18, 48).

Immobilized pH gradient two-dimensional electrophoresis (IPG-2DE). Protein samples were analyzed by two-dimensional electrophoresis by using the IPGPhor-2D system from Amersham Pharmacia Biotech. Acetone pellets were resuspended in 7 M urea–2 M thiourea–1% ASB-14. DTT was added to a concentration of 20 mM prior to loading onto the first dimension (immobilized pH gradient), along with the appropriate pH range immobilized pH gradient buffer (pH 3 to 10) at a concentration of 0.05%. Samples were included directly in the rehydration buffer and allowed to swell the immobilized pH gradient strip overnight (30 V, 20°C) or were loaded directly onto the swollen strip (18 cm) via cup loading. The isoelectric focusing parameters were as follows: (i) 1 min at a 500-V gradient, (ii) 1.5 h at a 4,000-V gradient, and (iii) 8,000 V for 40,000 V · h, with a 50-μA/strip maximum setting at 20°C. The completed first-dimension strip was separated by conventional SDS–12% PAGE, and the proteins were transferred to polyvinylidene difluoride for immunoblotting as described above.

RESULTS

Quantitation of *B. burgdorferi* in SCID mouse tissues. C3H SCID mice were infected with 1×10^7 *B. burgdorferi* B31 cells (passage two) and were sacrificed 17 days later, as described in Materials and Methods. In order to determine the number of

TABLE 1. Numbers of *B. burgdorferi* B31 cells in SCID mouse tissues as determined by RT-PCR

Tissue	No. of borrelia cells/μg of mouse DNA
Ear	$9.9 \times 10^4 \pm 4.0 \times 10^4$[a]
Ankle	$7.3 \times 10^4 \pm 1.3 \times 10^4$
Knee	$5.5 \times 10^4 \pm 1.7 \times 10^4$
Heart	$5.4 \times 10^4 \pm 1.2 \times 10^4$

[a] Mean ± standard error.

spirochetes present in infected tissues, RT-PCR was performed with samples of ears, ankles, knees, and hearts (Table 1). The values shown in Table 1 were derived from three separate animals and indicate that the tissues investigated contained 5,400 to 9,900 *Borrelia* cells per μg of mouse DNA. We estimated that these values correspond to approximately 1×10^5 to 5×10^5 *Borrelia* cells per ear, ankle, knee, or heart.

Extraction of HAB antigens from SCID mouse tissues by Triton X-114 phase partitioning. HAB antigens were extracted from the infected tissues (ear, ankle, knee, and heart) with Triton X-114, as described Materials and Methods. Triton X-114 detergent-phase-derived samples representing one-half of an individual tissue structure (ear, ankle, knee, or heart) were analyzed by SDS-PAGE and immunoblotted with serum from rabbits immune to reinfection (IRS) (17). Figure 1 shows the antigenic profiles of 10^5 IVCB cells and of HAB cells extracted from mouse ears, ankles, knees, and hearts. IRS detected OspA and OspB in 10^5 IVCB cells but did not detect OspA and OspB in the infected tissues. The antigenic profile of HAB is clearly distinct from that of IVCB. A band with the molecular mobility of VlsE (43 kDa) was detected in ear, ankle, and knee tissues but was not detected in heart tissue or in 10^5 IVCB cells. A band with the molecular mobility of OspC (22 kDa) was detected faintly in ear tissue and strongly in heart tissue. The identities of these bands were confirmed with monospecific VlsE and OspC antisera, as described below. Uninfected SCID mouse tissues that were processed identically did not react with IRS (data not shown).

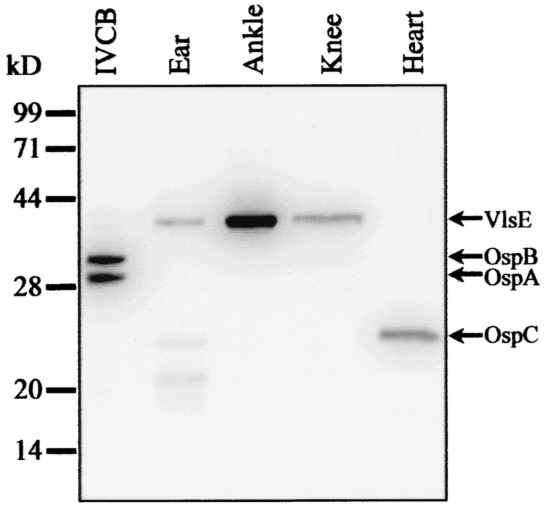

FIG. 1. Antigenic profiles of IVCB and HAB detected with IRS. Triton X-114 detergent-phase tissue samples from infected C3H SCID mice and detergent-phase IVCB controls were analyzed by SDS-PAGE and immunoblotting with IRS. A preparation containing 1×10^5 detergent-phase B31 cells was used for comparison.

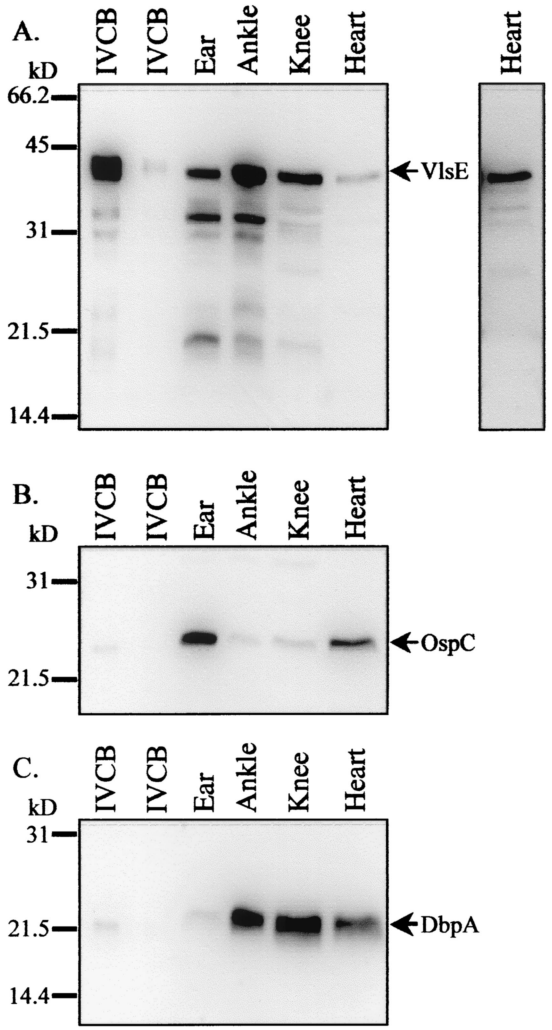

FIG. 2. Antigenic profiles of IVCB and HAB detected with monospecific antisera. Triton X-114 detergent-phase tissue samples from infected C3H SCID mice and detergent-phase IVCB controls were analyzed by SDS-PAGE and immunoblotted with the following monospecific antisera: VlsE (A), OspC (B), and DbpA (C). Preparations containing 5×10^6 and 5×10^5 detergent-phase B31 cells were used for comparison. In panel A the additional heart lane on the right is an overexposure.

Relative amounts of VlsE, DbpA, and OspC in infected tissues and IVCB. To assess the amounts of VlsE, DbpA, and OspC found in SCID mouse tissues relative to the amounts in IVCB, an immunoblot analysis was performed by using monospecific antisera, as shown in Fig. 2. As described above, the tissue samples analyzed each represented one-half of an individual tissue structure (ear, ankle, knee, heart). VlsE was readily detected in 5×10^6 IVCB cells but was barely detected in 5×10^5 IVCB cells (Fig. 2A). Both unit-size and smaller forms of VlsE were found in ear, ankle, and knee tissues and in 5×10^6 IVCB cells. The amount of VlsE detected in one-half a heart was similar to the amount found in 5×10^5 IVCB

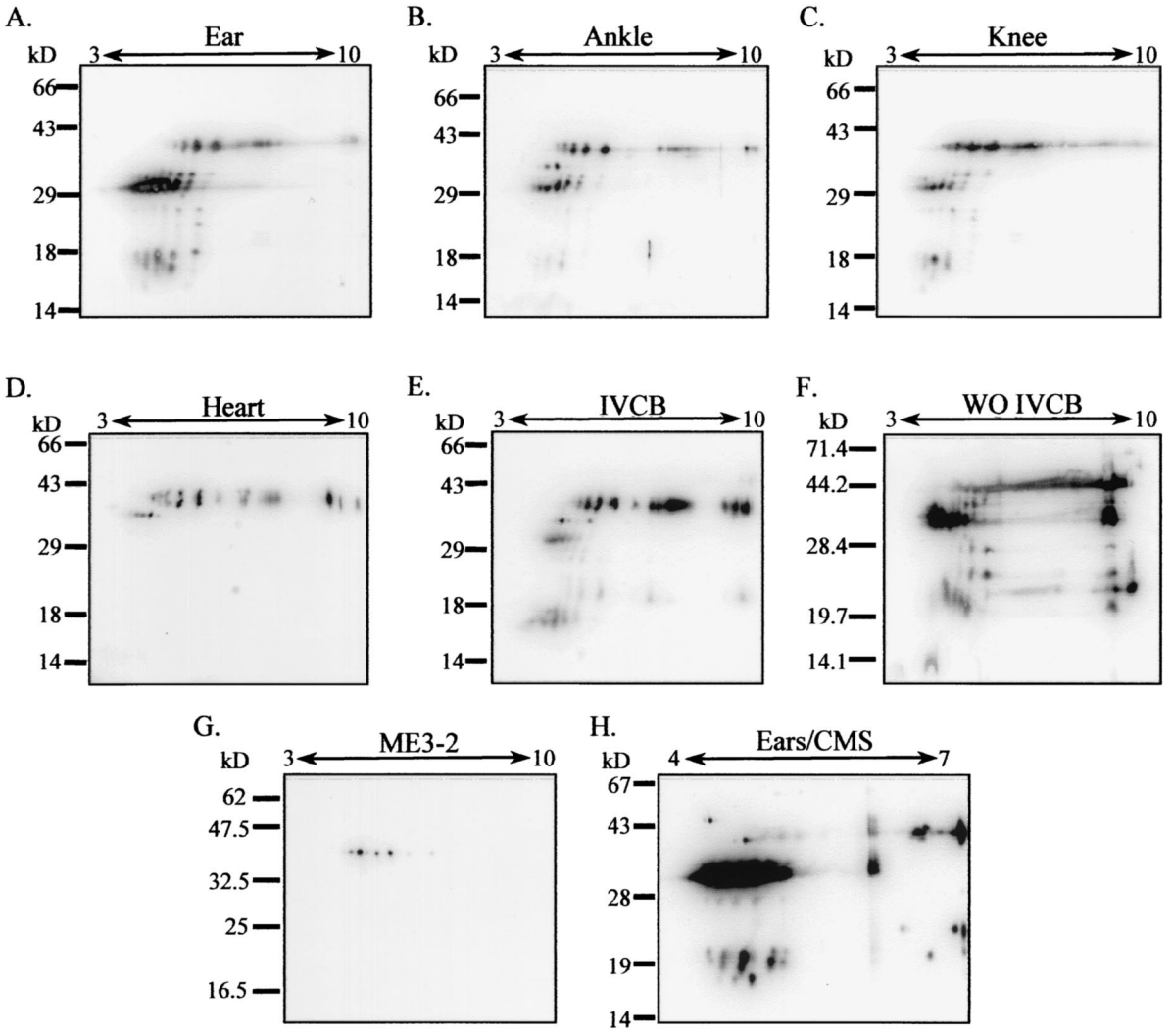

FIG. 3. Multiple sizes and isoforms of VlsE are present in IVCB and B31-infected C3H SCID mice. Triton X-114 detergent-phase tissue samples from infected C3H SCID mice and IVCB were analyzed by IPG-2DE and immunoblotted with monospecific VlsE antiserum. (A) Ear; (B) knee; (C) ankle; (D) heart; (E) 1×10^9 B31 detergent-phase cells; (F) 1×10^9 B31 whole organisms; (G) 1×10^9 ME3-2 detergent-phase cells; (H) ear, probed with CMS.

cells. Given the numbers of HAB cells detected in knees (Table 1), it is clear that VlsE is much more abundant in HAB cells found in knee tissues than in a corresponding number of IVCB cells. While IVCB and HAB both contained smaller VlsE forms whose sizes were similar, the relative proportion of the smaller forms of VlsE detected in the ear and ankle tissue samples was greater than in IVCB. In conditions under which OspC was barely detected in 5×10^6 IVCB cells and was not detected in 5×10^5 IVCB cells, it was readily detected in the comparable numbers of HAB cells found in heart tissue and was also prominent in ear tissue (Fig. 2B). In conditions under which DbpA was barely detectable in 5×10^6 IVCB cells and was undetectable in 5×10^5 IVCB cells, it was readily detected in all the infected tissues except the ear (Fig. 2C). Uninfected SCID mouse tissues that were processed identically did not react with IRS (data not shown).

Multiple sizes and isoforms of VlsE in tissue samples and IVCB. VlsE is known to undergo antigenic variation during infection (60). To assess the number of VlsE isoforms in tissues and to further characterize the smaller forms of VlsE whose existence was revealed by the one-dimensional immunoblot shown in Fig. 2A, the SCID mouse tissue samples were analyzed by IPG-2DE (Fig. 3). Monospecific polyclonal VlsE antiserum detected multiple isoforms of unit-size VlsE in IVCB and in each of the tissue samples. It should be noted that the B31 strain used to infect the mice was not clonal with regard to the *vlsE* loci. Smaller forms of VlsE were also found in each of the tissue samples (Fig. 3A to D) and in IVCB (Fig. 3E). Like unit-size VlsE, the smaller forms were also present as multiple isoforms. The relative amounts of the lower-molecular-mass forms varied among the tissue samples; ear tissue contained the highest proportion of the lower-molecular-mass forms rel-

ative to unit-size VlsE, and heart tissue contained the lowest proportion of the lower-molecular-mass forms relative to unit-size VlsE. The smaller VlsE forms that were readily detected with VlsE antiserum were not detected with IRS (Fig. 1).

In order to determine if the smaller forms of VlsE were artifacts of the extraction process, intact IVCB cells were solubilized directly in buffer containing 7 M urea, 2 M thiourea, and 1% ASB-14 for analysis by IPG-2DE. As shown in Fig. 3F, smaller VlsE forms were readily detected. To determine if the smaller forms of VlsE were the result of cross-reactivity between the sera and *Borrelia* proteins other than VlsE, a B31 clonal isolate, ME3-2, which lacks linear plasmid 28.1 and therefore cannot express *vlsE*, was also analyzed with the monospecific VlsE antiserum (Fig. 3G). After a longer exposure (10 min, compared with 1 to 2 min for the other samples) only a single species was observed around 40 kDa, which did not correspond to unit-size VlsE or its smaller forms. Because immune rabbit serum did not bind the smaller VlsE forms (Fig. 1), we probed an immunoblot of ear tissue infected with CMS. The pattern of reactivity of CMS with infected ear tissue (Fig. 3I) showed striking overlap with the pattern of reactivity of the rabbit polyclonal monospecific VlsE antiserum with ear tissue (Fig. 3A). The smaller forms of VlsE were also found in infected rabbit skin and were detectable with CMS (data not shown).

Relative amounts of *vlsE*, *dbpA*, and *ospC* transcripts in HAB and IVCB. The findings presented above provide a measure of the relative amounts of VlsE, DbpA, and OspC found in SCID mouse tissues and in IVCB. We also determined the relative amounts of the transcripts by RT-PCR as described in Materials and Methods. IVCB cells were added to normal mouse tissue and processed in the same way as the infected tissue (Fig. 4). In conditions under which approximately equal amounts of the *flaB* product were detected in IVCB and in infected ear, knee, ankle, and heart tissues, *vlsE*, *ospC*, and *dbpA* products were detected in the infected tissues but not in identically processed IVCB. These findings indicate that transcription of these genes is upregulated during infection. *ospC* and *dbpA* products were most prominently detected in infected ankle and ear tissues, respectively. The relative amounts of *vlsE*, *ospC*, and *dbpA* transcripts with respect to each other varied considerably from tissue to tissue in conditions under which *flaB* detection was constant. The amount of *dbpA* transcripts in ear tissue was not in accord with the relative paucity of DbpA detected in ear tissue by immunoblotting (Fig. 2C).

HAB antigenic composition revealed by IPG-2DE and immunoblotting with IRS. In the experiments described above we assessed the process of *B. burgdorferi* host adaptation insofar as it extends to OspA, OspB, VlsE, DbpA, and OspC, surface proteins that have been the focus of extensive study by workers in the *Borrelia* field. Our findings are the first direct demonstration that the amount of VlsE is markedly increased relative to the amount in IVCB, a finding that is not surprising given the possible importance of VlsE as a virulence factor during infection (29, 41). To obtain a broader view of the antigenic changes that comprise host adaptation, we analyzed SCID mouse tissues, extracted with Triton X-114 as described in Materials and Methods, by IPG-2DE and immunoblotting with IRS. Figure 5 shows the antigenic profiles of 10^7 IVCB cells and of ear samples (derived from 10 ears), ankle samples (derived from 2.5 ankles), and heart samples (derived from two hearts), as determined by probing immunoblots with IRS. OspA and OspB were the most prominent hydrophobic constituents of IVCB detected with IRS (Fig. 5A). OspA and OspB were not detected in any of the tissue samples (Fig. 5B to D). The positions of BmpA, OspC, and LA7 were determined by probing parallel tissue immunoblots with the individual monospecific antisera; spot matching was performed with ImageMaster software (APBiotech). These individual monospecific sera were found to react with only a single band when they were used to probe an immunoblot of IVCB cells separated by SDS-PAGE. The gene encoding BmpA (basic membrane protein A) is part of a cluster of paralogous genes whose function is unknown (14, 49, 50). LA7, originally identified as a *Borrelia* antigen that is reactive with a monoclonal antibody, is a lipoprotein that is believed to be localized to the

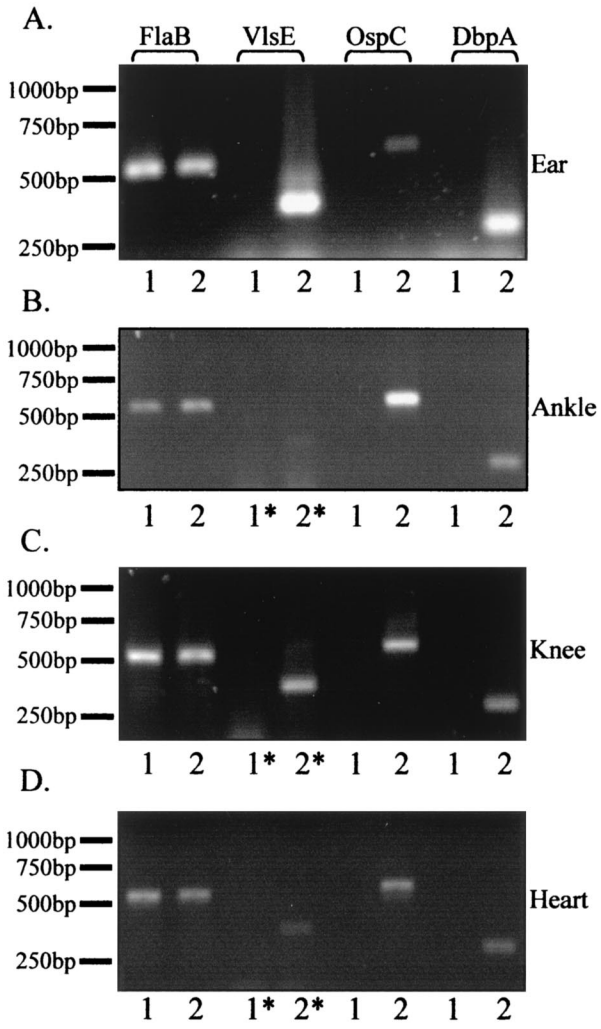

FIG. 4. Amounts of *vlsE*, *dbpA*, and *ospC* transcripts in infected SCID mouse tissues and IVCB. RT-PCR was performed to identify the transcripts. IVCB controls were normalized to provide an amount of *flaB* transcripts approximately equal to the amount in each infected tissue sample. (A) Ear; (B) ankle; (C) knee; (D) heart. Lanes 1, IVCB control; lanes 2, infected tissue. An asterisk indicates that 45 cycles were used; 40 cycles were used for the other samples.

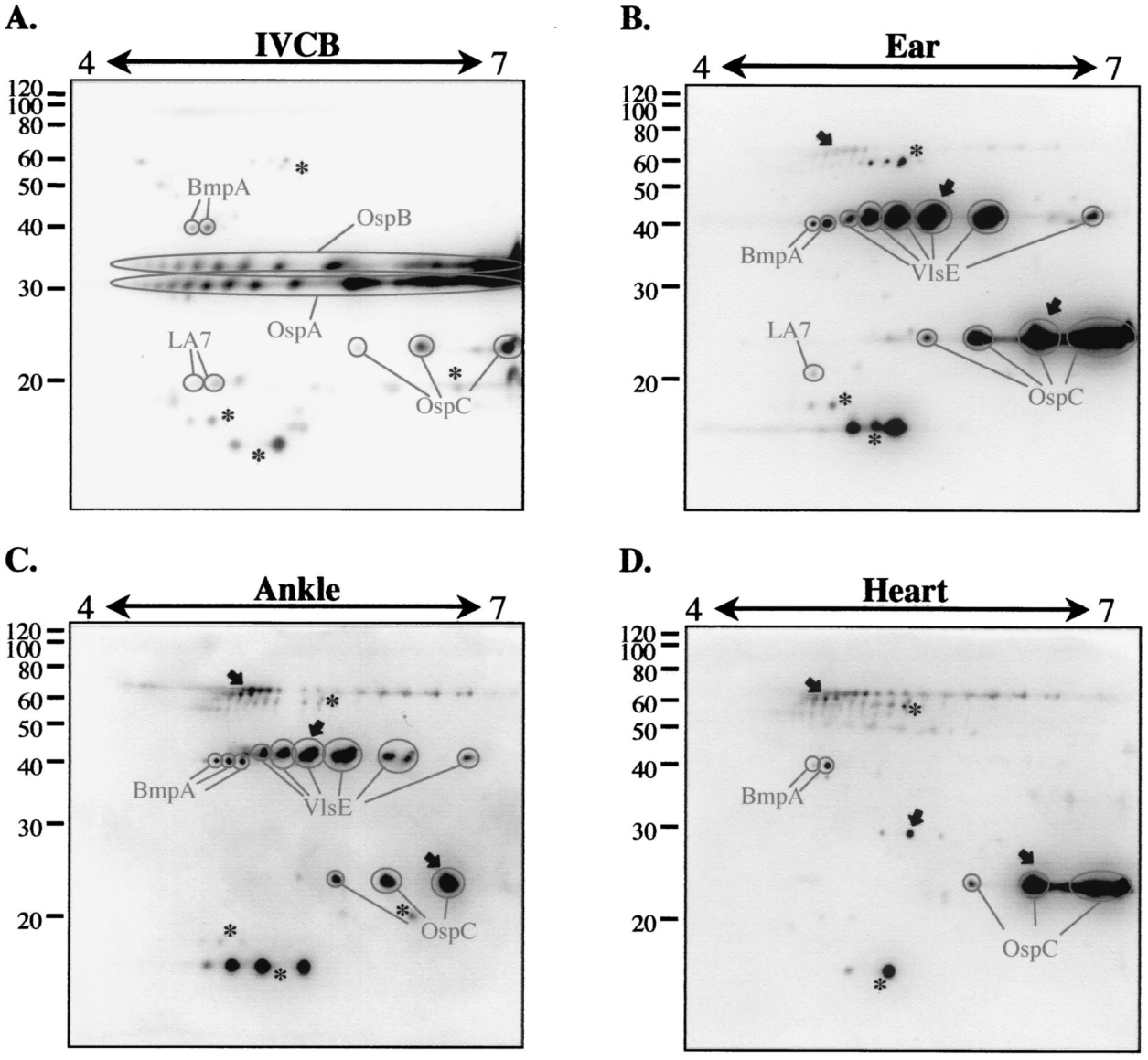

FIG. 5. Antigenic composition of HAB. Triton X-114 detergent-phase samples derived from the tissues of infected C3H SCID mice and IVCB were analyzed by using IPG-2DE and immunoblotting with IRS. The arrows indicate antigens that appear to be upregulated in tissue. The asterisks indicate unidentified proteins found in both tissue and IVCB.

outer membrane (19, 27, 56). The function of this protein has not been determined yet. IRS detected prominent unit-size VlsE isoforms in ear and ankle tissues. (IRS, as shown above, does not bind the smaller forms of VlsE in two-dimensional immunoblots, and CMS strongly binds the smaller VlsE forms found in ear tissue, as shown in Fig. 3I.) The failure of IRS to detect VlsE in heart tissue was striking and corroborates the immunoblot findings shown in Fig. 1 and 2 obtained with monospecific VlsE antiserum. OspC was the most prominent antigen found in heart tissue. IRS detected BmpA in IVCB and in ear, ankle, and heart tissues. IRS detected LA7 in IVCB and in ear tissue. IRS detected an approximately 65-kDa antigen in ear, ankle, and heart tissues but not in IVCB. It appears that there are many isoforms of this antigen, and it is possible that more than one protein reacts with the IRS. Heart tissue contained a novel 30-kDa antigen not detected by IRS in IVCB.

In addition to these proteins that appear to be upregulated during mammalian infection, IRS reacted with antigens found in both IVCB and tissues; these antigens had molecular masses of 58, 18.9, 16.7, and 14.8 kDa (Fig. 5). The 14.8-kDa antigen is particularly reactive in both IVCB and tissue. The identities of these protein species are unknown, and the proteins are being studied. Uninfected SCID mouse tissues processed identically were probed with IRS, and no cross-reactivity was found (data not shown). Additionally, normal rabbit skin spiked with

IVCB cells and processed in the same manner showed no difference in IRS reactivity when it was compared with IVCB cells alone (data not shown).

DISCUSSION

Understanding the membrane protein changes that *B. burgdorferi* undergoes after transmission to vertebrate hosts has become an important goal of Lyme disease research. Underscoring the importance of this goal is the fact that immunity to challenge with IVCB does not necessarily correspond to immunity to HAB in mice (4) and rabbits (47). The fact that relatively small numbers of spirochetes are present in the tissues of infected mice (2, 35, 57) has been a significant obstacle to direct compositional analysis of HAB. No method has been described to release intact spirochetes from tissue. Montgomery et al. recovered HAB from mice by peritoneal lavage and reported detection of surface OspC by immunofluorescence (37). There has been no other such direct analysis of HAB surface antigenic structure. Microarray technology has been used recently to explore differential expression of *B. burgdorferi* genes under different environmental conditions during in vitro cultivation (33, 45). In a recent elegant study, Fikrig and colleagues used a microarray system to assess expression of 137 genes encoding lipoproteins in immunodeficient and immunocompetent mice (34). All but 40 of these genes were downregulated after infection in immunocompetent mice, presumably as a response to host immunity.

In this report, we describe a novel approach for determining the hydrophobic antigen composition of HAB in infected tissue. This approach, termed hydrophobic antigen tissue Triton extraction (HATTREX), was used to determine the amounts of VlsE, DbpA, and OspC in tissue in relation to the relative amounts in IVCB. HATTREX is based on the fact that most *B. burgdorferi* membrane proteins are hydrophobic (52), although there are exceptions, such as the channel-forming protein P66 (Oms66) (51), which is believed to be an integrin binding protein (9). Triton X-114 phase partitioning has been employed for a long time to obtain a membrane protein-enriched fraction from pathogenic spirochetes (11, 42, 43). In this study, Triton X-114 extraction of infected SCID mouse tissues followed by phase partitioning proved to be a remarkably effective way of concentrating the small numbers of HAB cells (about 10^5 spirochetes) found in individual biological structures, such as a mouse heart, ear, ankle, or knee joint, for antigenic analysis by immunoblotting. HATTREX works because only a small proportion of mouse tissue proteins are hydrophobic, whereas most HAB antigens of interest are hydrophobic. Analysis of HAB antigens in the hydrophilic or aqueous phase has been problematic because the large amount of mouse protein relative to the amount of HAB hydrophilic protein can result in overloading of gels. The findings presented here were restricted to analysis of hydrophobic detergent-phase antigens. Because flagellin is a hydrophilic protein, it could not be included as a reference for a protein whose abundance should be constant under different environmental conditions. It should also be noted that a limitation of conclusions that can be drawn after use of HATTREX is related to the fact that this method is a method for determining antigenic composition and does not assess the antigenic structure of the intact spirochete. Cox and colleagues have shown that the surface exposure of OspA is far less than its compositional abundance suggests (10). Abundance, as shown by HATTREX and immunoblotting, does not differentiate between surface and subsurface hydrophobic antigens. It is also conceivable that some proportion of the antigens detected by HATTREX could have an extracellular location (for example, in the form of membrane blebs).

At this time, OspC (23, 28, 31), DbpA (6, 22, 23), and the antigenic variation protein VlsE (15, 24, 32, 39) are the most intensively studied *B. burgdorferi* membrane proteins. While it has been established that VlsE antigenic variation occurs only during mammalian infection (24) and that the VlsE-encoding plasmid Lp28-1 is important to the virulence of *B. burgdorferi* during infection of mice (29, 41), VlsE is not an abundant constituent of IVCB, and there have been no reports of the degree of VlsE expression during infection. The hydrophobic antigen composition of HAB revealed by the HATTREX approach is distinctly different from that of IVCB. HAB cells lack detectable OspA and OspB. In this regard our findings are not in accord with a recent report which demonstrated that *ospB* transcripts are present throughout infection of immunodeficient mice (34). It is striking that VlsE is the most abundant hydrophobic antigen of HAB extracted from ear and joint tissues, as judged by immunoblotting with IRS, while it is an undetectable constituent of IVCB probed with the same antiserum under identical conditions. Equally striking is the consistent observation in three separate experiments of the paucity of VlsE in heart tissue. One possible explanation for this could be the presence of a protease in the heart tissue that is not as abundant as it is in other tissues. Alternatively, regulation of VlsE could be tissue specific. It will be interesting to ascertain the level of VlsE expression in the hearts of immunocompetent mice. While OspC is a prominent constituent of HAB in SCID mouse ear, heart, and joint tissues, Liang and colleagues have shown that OspC synthesis decreases in response to the development of specific antibodies by immunocompetent mice, as discussed below (31).

The antigenic profiles of HAB provide a relative indication of spirochetal proteins that are far more abundant than they are in IVCB. While we and other workers have estimated the numbers of *B. burgdorferi* cells in infected tissues by PCR (47, 57), the estimates are based on the assumption that there is one copy of the chromosome per spirochete (38). There is no information about the chromosome content of HAB.

We also employed RT-PCR as a means of determining whether there was correspondence between the amount of an antigen in infected tissues as detected by HATTREX and the amount of the antigen in infected tissues as detected by immunoblotting. An advantage of the RT-PCR approach was its ability to provide an internal control for a gene whose expression was unlikely to be environmentally regulated, the gene encoding the flagellar subunit protein, *flaB*. This hydrophilic protein could not be recovered by HATTREX. When RT-PCR was used and HAB and IVCB samples were normalized relative to the amount of *flaB* present in each sample, the higher levels of *vlsE*, *dbpA*, and *ospC* RT-PCR transcripts in HAB than in IVCB were apparent, just as HATTREX revealed larger amounts of VlsE, DbpA, and OspC in HAB cells than in similar numbers of IVCB cells. HATTREX-immuno-

blotting and RT-PCR findings diverged, however, with regard to tissue-specific differences in the amounts of the antigens or their transcripts relative to each other. For example, the relative amount of the *dbpA* transcript in ear tissue was greater than the amount of DbpA relative to OspC and VlsE. However, it should be emphasized that all these antigens and transcripts are abundant in tissues relative to the amounts in IVCB. The role of tissue-specific differences in abundance is of potential interest for pathogenesis but is conjectural at this time. It has been shown that *dbpA* synthesis and *ospC* synthesis are coordinately regulated by RpoN-RpoS in vitro (23). In vivo expression may be multifactorial and tissue specific.

Recently, Liang et al. used RT-PCR to study the temporal expression of *ospC* in normal and SCID mice (31). *ospC* transcription is upregulated in SCID mice compared with transcription in IVCB. In normal mice, *ospC* transcription decreases in conjunction with the appearance of OspC antibodies. Infusion of OspC antibodies into SCID mice eliminated *ospC* transcription. In our work with SCID mice, *ospC* was clearly upregulated at the time point studied, 17 days after infection. We used HATTREX to examine the temporal expression of *B. burgdorferi* antigens in the skin of rabbits. In this case, the amount of *ospC* expressed was diminished in the same time frame as that described by Liang et al. for mice (31; T. Crother, C. Champion, J. Whitelegge, X. Wu, D. Blanco, J. Miller, and M. Lovett, unpublished data).

The amount of VlsE in HAB found during infection of SCID mice complements previous findings that VlsE undergoes antigenic variation during SCID mouse infection (60). Although VlsE appears to have a likely role in immune evasion through antigenic variation, initiation of VlsE antigenic variation does not seem to be dependent on an active immune system (29, 41, 60). It has been suggested that the gamma interferon pathway may be involved in activating VlsE recombination (3).

The lower-molecular-mass forms of VlsE, although present at minor levels in IVCB, are a striking feature of HAB in all mouse tissues except heart. Because the smaller VlsE forms are hydrophobic, as judged by isolation from the Triton X-114 detergent phase, it can be concluded that the hydrophobicity is due to retention of amino-terminal acylation. The predicted sequence topology of VlsE does not include membrane-spanning domains that would convey hydrophobicity (58). Therefore, it is likely that the smaller VlsE forms are generated by C-terminal proteolysis. This proteolysis appears to be of a specific nature, given the discrete molecular mobilities of the smaller VlsE forms. Smaller forms of the other abundant surface proteins, OspC and DbpA, were not found in the mouse tissue samples or in IVCB, arguing against generalized proteolytic degradation of surface proteins. It should be noted that smaller forms of OspA and OspB were not detected in IVCB (Fig. 5), while the smaller VlsE forms were readily detected in IVCB (Fig. 3E and F). The fact that smaller VlsE forms are found in IVCB supports the hypothesis that they are generated by a specific *B. burgdorferi* protease and do not reflect an autolytic activity of infected tissue.

Several additional lines of evidence are in accord with the possibility that the smaller VlsE forms are specifically produced by *B. burgdorferi* and are not artifactual. To assess the possibility that the smaller VlsE forms were generated by the Triton X-114 extraction process, intact IVCB cells were directly solubilized in sample buffer containing 7 M urea, 2 M thiourea, and 1% ASB-14 prior to IPG-2DE. The smaller VlsE forms were readily detected (Fig. 3F). To assess the possibility that the smaller VlsE forms represented cross-reactions of the smaller VlsE form monospecific antiserum with other *B. burgdorferi* proteins, we analyzed a clonal isolate of *B. burgdorferi* that lacked Lp28.1 and was therefore unable to express VlsE. Smaller VlsE form bands were not detected, indicating that the binding of the VlsE antiserum to smaller VlsE forms was specific (Fig. 3G). Because the monospecific VlsE antiserum was generated by immunization with recombinant VlsE, we considered the possibility that its ability to bind smaller VlsE forms reflected immunization with breakdown products of recombinant VlsE. We found, however, that serum from mice chronically infected with *B. burgdorferi* (CMS) also bound the smaller VlsE forms (Fig. 3I).

Apart from specific proteolysis, another possible route for generation of the smaller VlsE forms is by illegitimate recombination events during antigenic variation. However, no truncated *vlsE* open reading frames have been found in the numerous studies performed on VlsE (24, 25, 58, 59). Furthermore, analysis of VlsE in several individual clonal isolates of B31 revealed both unit-size VlsE and smaller VlsE forms (Crother and Lovett, unpublished observations). Taken together, our data suggest that *B. burgdorferi* produces smaller VlsE forms through a specific mechanism both during infection and during in vitro cultivation.

There has been one previous study in which smaller forms of a *B. burgdorferi* surface protein were detected. Bundoc and Barbour found that clonal isolates of strain HB19 expressed different forms of OspB (5). Some clones expressed unit-size (33-kDa) OspB, some expressed both 33-kDa OspB and a 21-kDa form of OspB, and others expressed only an 18.5-kDa form of OspB. The mechanistic basis for these modes of OspB expression was not determined. Our studies did not reveal smaller forms of OspB in IVCB cells of strain B31 (Fig. 5), and OspB was not detected in HAB. In addition, we analyzed VlsE forms from clonal isolates of strain B31 (data not shown), and each clone contained the full set of smaller VlsE forms shown in Fig. 3. The smaller VlsE forms therefore do not appear to be expressed as a result of clonal variation.

The crystal structure of VlsE has recently been described (15). Precise determination of VlsE cleavage sites in relation to the topology is of great interest and may provide an indication of whether the protein is cleaved prior to export and mature folding. It seems highly likely that the cleavage events greatly change VlsE topology. As such, VlsE processing and creation of smaller VlsE forms could be yet another means by which *B. burgdorferi* can evade the immune response.

It is noteworthy that the antigenic profile of HAB obtained by HATTREX, while dominated in ear and joint tissues by VlsE, contains novel antigens that are upregulated relative to their representation in IVCB. The cellular location and biological significance of these proteins remain to be determined. Using the HATTREX approach, we also identified proteins, such as LA7 and BmpA, which are readily detectable but not massively upregulated in certain tissues, as well as in IVCB. The use of complementary methodological approaches to ascertain HAB gene expression and antigenic composition dur-

ing infection is clearly indicated given both the difficulty of obtaining this information and its importance.

ACKNOWLEDGMENTS

This research was funded by NIH grants AI 29733 and AI 37312. We thank Evelyn Pineda for her invaluable assistance.

REFERENCES

1. **Akins, D. R., S. F. Porcella, T. G. Popova, D. Shevchenko, S. I. Baker, M. Li, M. V. Norgard, and J. D. Radolf.** 1995. Evidence for *in vivo* but not *in vitro* expression of a *Borrelia burgdorferi* outer surface protein F (OspF) homologue. Mol. Microbiol. **18:**507–520.
2. **Anguita, J., S. Samanta, B. Revilla, K. Suk, S. Das, S. W. Barthold, and E. Fikrig.** 2000. *Borrelia burgdorferi* gene expression in vivo and spirochete pathogenicity. Infect. Immun. **68:**1222–1230.
3. **Anguita, J., V. Thomas, S. Samanta, R. Persinski, C. Hernanz, S. W. Barthold, and E. Fikrig.** 2001. *Borrelia burgdorferi*-induced inflammation facilitates spirochete adaptation and variable major protein-like sequence locus recombination. J. Immunol. **167:**3383–3390.
4. **Barthold, S. W., E. Fikrig, L. K. Bockenstedt, and D. H. Persing.** 1995. Circumvention of outer surface protein A immunity by host-adapted *Borrelia burgdorferi*. Infect. Immun. **63:**2255–2261.
5. **Bundoc, V. G., and A. G. Barbour.** 1989. Clonal polymorphisms of outer membrane protein OspB of *Borrelia burgdorferi*. Infect. Immun. **57:**2733–2741.
6. **Cassatt, D. R., N. K. Patel, N. D. Ulbrandt, and M. S. Hanson.** 1998. DbpA, but not OspA, is expressed by *Borrelia burgdorferi* during spirochetemia and is a target for protective antibodies. Infect. Immun. **66:**5379–5387.
7. **Champion, C. I., D. R. Blanco, J. T. Skare, D. A. Haake, M. Giladi, D. Foley, J. N. Miller, and M. A. Lovett.** 1994. A 9.0-kilobase-pair circular plasmid of *Borrelia burgdorferi* encodes an exported protein: evidence for expression only during infection. Infect. Immun. **62:**2653–2661.
8. **Chevallet, M., V. Santoni, A. Poinas, D. Rouquie, A. Fuchs, S. Kieffer, M. Rossignol, J. Lunardi, J. Garin, and T. Rabilloud.** 1998. New zwitterionic detergents improve the analysis of membrane proteins by two-dimensional electrophoresis. Electrophoresis **19:**1901–1909.
9. **Coburn, J., W. Chege, L. Magoun, S. C. Bodary, and J. M. Leong.** 1999. Characterization of a candidate *Borrelia burgdorferi* beta3-chain integrin ligand identified using a phage display library. Mol. Microbiol. **34:**926–940.
10. **Cox, D. L., D. R. Akins, K. W. Bourell, P. Lahdenne, M. V. Norgard, and J. D. Radolf.** 1996. Limited surface exposure of *Borrelia burgdorferi* outer surface lipoproteins. Proc. Natl. Acad. Sci. USA **93:**7973–7978.
11. **Cunningham, T. M., E. M. Walker, J. N. Miller, and M. A. Lovett.** 1988. Selective release of the *Treponema pallidum* outer membrane and associated polypeptides with Triton X-114. J. Bacteriol. **170:**5789–5796.
12. **Das, S., S. W. Barthold, S. S. Giles, R. R. Montgomery, S. R. Telford 3rd, and E. Fikrig.** 1997. Temporal pattern of *Borrelia burgdorferi* p21 expression in ticks and the mammalian host. J. Clin. Investig. **99:**987–995.
13. **de Silva, A. M., S. R. Telford 3rd, L. R. Brunet, S. W. Barthold, and E. Fikrig.** 1996. *Borrelia burgdorferi* OspA is an arthropod-specific transmission-blocking Lyme disease vaccine. J. Exp. Med. **183:**271–275.
14. **Dobrikova, E. Y., J. Bugrysheva, and F. C. Cabello.** 2001. Two independent transcriptional units control the complex and simultaneous expression of the *bmp* paralogous chromosomal gene family in *Borrelia burgdorferi*. Mol. Microbiol. **39:**370–378.
15. **Eicken, C., V. Sharma, T. Klabunde, M. B. Lawrenz, J. M. Hardham, S. J. Norris, and J. C. Sacchettini.** 2002. Crystal structure of Lyme disease variable surface antigen VlsE of *Borrelia burgdorferi*. J. Biol. Chem. **28:**28.
16. **Fikrig, E., W. Feng, S. W. Barthold, S. R. Telford 3rd, and R. A. Flavell.** 2000. Arthropod- and host-specific *Borrelia burgdorferi bbk32* expression and the inhibition of spirochete transmission. J. Immunol. **164:**5344–5351.
17. **Foley, D. M., R. J. Gayek, J. T. Skare, E. A. Wagar, C. I. Champion, D. R. Blanco, M. A. Lovett, and J. N. Miller.** 1995. Rabbit model of Lyme borreliosis: erythema migrans, infection-derived immunity, and identification of *Borrelia burgdorferi* proteins associated with virulence and protective immunity. J. Clin. Investig. **96:**965–975.
18. **Foley, D. M., Y. P. Wang, X. Y. Wu, D. R. Blanco, M. A. Lovett, and J. N. Miller.** 1997. Acquired resistance to *Borrelia burgdorferi* infection in the rabbit. Comparison between outer surface protein A vaccine- and infection-derived immunity. J. Clin. Investig. **99:**2030–2035.
19. **Grewe, C., and J. H. Nuske.** 1996. Immunolocalization of a 22 kDa protein (IPLA7, P22) of *Borrelia burgdorferi*. FEMS Microbiol. Lett. **138:**215–219.
20. **Guo, B. P., E. L. Brown, D. W. Dorward, L. C. Rosenberg, and M. Hook.** 1998. Decorin-binding adhesins from *Borrelia burgdorferi*. Mol. Microbiol. **30:**711–723.
21. **Guo, B. P., S. J. Norris, L. C. Rosenberg, and M. Hook.** 1995. Adherence of *Borrelia burgdorferi* to the proteoglycan decorin. Infect. Immun. **63:**3467–3472.
22. **Hagman, K. E., X. Yang, S. K. Wikel, G. B. Schoeler, M. J. Caimano, J. D. Radolf, and M. V. Norgard.** 2000. Decorin-binding protein A (DbpA) of *Borrelia burgdorferi* is not protective when immunized mice are challenged via tick infestation and correlates with the lack of DbpA expression by *B. burgdorferi* in ticks. Infect. Immun. **68:**4759–4764.
23. **Hubner, A., X. Yang, D. M. Nolen, T. G. Popova, F. C. Cabello, and M. V. Norgard.** 2001. Expression of *Borrelia burgdorferi* OspC and DbpA is controlled by a RpoN-RpoS regulatory pathway. Proc. Natl. Acad. Sci. USA **98:**12724–12729.
24. **Indest, K. J., J. K. Howell, M. B. Jacobs, D. Scholl-Meeker, S. J. Norris, and M. T. Philipp.** 2001. Analysis of *Borrelia burgdorferi vlsE* gene expression and recombination in the tick vector. Infect. Immun. **69:**7083–7090.
25. **Iyer, R., J. M. Hardham, G. P. Wormser, I. Schwartz, and S. J. Norris.** 2000. Conservation and heterogeneity of *vlsE* among human and tick isolates of *Borrelia burgdorferi*. Infect. Immun. **68:**1714–1718.
26. **Kitten, T., and A. G. Barbour.** 1992. The relapsing fever agent *Borrelia hermsii* has multiple copies of its chromosome and linear plasmids. Genetics **132:**311–324.
27. **Kramer, M. D., U. E. Schaible, R. Wallich, S. E. Moter, D. Petzoldt, and M. M. Simon.** 1990. Characterization of *Borrelia burgdorferi* associated antigens by monoclonal antibodies. Immunobiology **181:**357–366.
28. **Kumaran, D., S. Eswaramoorthy, B. J. Luft, S. Koide, J. J. Dunn, C. L. Lawson, and S. Swaminathan.** 2001. Crystal structure of outer surface protein C (OspC) from the Lyme disease spirochete, *Borrelia burgdorferi.* EMBO J. **20:**971–978.
29. **Labandeira-Rey, M., and J. T. Skare.** 2001. Decreased infectivity in *Borrelia burgdorferi* strain B31 is associated with loss of linear plasmid 25 or 28–1. Infect. Immun. **69:**446–455.
30. **Laemmli, U. K.** 1970. Cleavage of structural proteins during the assembly of the head of bacteriophage T4. Nature **227:**680–685.
31. **Liang, F. T., M. B. Jacobs, L. C. Bowers, and M. T. Philipp.** 2002. An immune evasion mechanism for spirochetal persistence in lyme borreliosis. J. Exp. Med. **195:**415–422.
32. **Liang, F. T., M. B. Jacobs, and M. T. Philipp.** 2001. C-terminal invariable domain of VlsE may not serve as target for protective immune response against *Borrelia burgdorferi*. Infect. Immun. **69:**1337–1343.
33. **Liang, F. T., F. K. Nelson, and E. Fikrig.** 2002. DNA microarray assessment of putative *Borrelia burgdorferi* lipoprotein genes. Infect. Immun. **70:**3300–3303.
34. **Liang, F. T., F. K. Nelson, and E. Fikrig.** 2002. Molecular adaptation of *Borrelia burgdorferi* in the murine host. J. Exp. Med. **196:**275–280.
35. **Ma, Y., K. P. Seiler, E. J. Eichwald, J. H. Weis, C. Teuscher, and J. J. Weis.** 1998. Distinct characteristics of resistance to *Borrelia burgdorferi*-induced arthritis in C57BL/6N mice. Infect. Immun. **66:**161–168.
36. **Molloy, M. P., B. R. Herbert, M. B. Slade, T. Rabilloud, A. S. Nouwens, K. L. Williams, and A. A. Gooley.** 2000. Proteomic analysis of the *Escherichia coli* outer membrane. Eur. J. Biochem. **267:**2871–2881.
37. **Montgomery, R. R., S. E. Malawista, K. J. Feen, and L. K. Bockenstedt.** 1996. Direct demonstration of antigenic substitution of *Borrelia burgdorferi ex vivo*: exploration of the paradox of the early immune response to outer surface proteins A and C in Lyme disease. J. Exp. Med. **183:**261–269.
38. **Morrison, T. B., Y. Ma, J. H. Weis, and J. J. Weis.** 1999. Rapid and sensitive quantification of *Borrelia burgdorferi*-infected mouse tissues by continuous fluorescent monitoring of PCR. J. Clin. Microbiol. **37:**987–992.
39. **Philipp, M. T., L. C. Bowers, P. T. Fawcett, M. B. Jacobs, F. T. Liang, A. R. Marques, P. D. Mitchell, J. E. Purcell, M. S. Ratterree, and R. K. Straubinger.** 2001. Antibody response to IR6, a conserved immunodominant region of the VlsE lipoprotein, wanes rapidly after antibiotic treatment of *Borrelia burgdorferi* infection in experimental animals and in humans. J. Infect. Dis. **184:**870–878.
40. **Probert, W. S., and B. J. Johnson.** 1998. Identification of a 47 kDa fibronectin-binding protein expressed by *Borrelia burgdorferi* isolate B31. Mol. Microbiol. **30:**1003–1015.
41. **Purser, J. E., and S. J. Norris.** 2000. Correlation between plasmid content and infectivity in *Borrelia burgdorferi*. Proc. Natl. Acad. Sci. USA **97:**13865–13870.
42. **Radolf, J. D., N. R. Chamberlain, A. Clausell, and M. V. Norgard.** 1988. Identification and localization of integral membrane proteins of virulent *Treponema pallidum* subsp. *pallidum* by phase partitioning with the nonionic detergent Triton X-114. Infect. Immun. **56:**490–498.
43. **Radolf, J. D., and M. V. Norgard.** 1988. Pathogen specificity of *Treponema pallidum* subsp. *pallidum* integral membrane proteins identified by phase partitioning with Triton X-114. Infect. Immun. **56:**1825–1828.
44. **Remington, M. C., E. L. Munson, S. M. Callister, M. L. Molitor, J. A. Christopherson, D. J. DeCoster, S. D. Lovrich, and R. F. Schell.** 2001. Interleukin-6 enhances production of anti-OspC immunoglobulin G2b borreliacidal antibody. Infect. Immun. **69:**4268–4275.
45. **Revel, A. T., A. M. Talaat, and M. V. Norgard.** 2002. DNA microarray analysis of differential gene expression in *Borrelia burgdorferi*, the Lyme disease spirochete. Proc. Natl. Acad. Sci. USA **99:**1562–1567.
46. **Schwan, T. G., J. Piesman, W. T. Golde, M. C. Dolan, and P. A. Rosa.** 1995. Induction of an outer surface protein on *Borrelia burgdorferi* during tick feeding. Proc. Natl. Acad. Sci. USA **92:**2909–2913.
47. **Shang, E. S., C. I. Champion, X. Y. Wu, J. T. Skare, D. R. Blanco, J. N. Miller, and M. A. Lovett.** 2000. Comparison of protection in rabbits against

host-adapted and cultivated *Borrelia burgdorferi* following infection-derived immunity or immunization with outer membrane vesicles or outer surface protein A. Infect. Immun. **68:**4189–4199.
48. **Shang, E. S., X. Y. Wu, M. A. Lovett, J. N. Miller, and D. R. Blanco.** 2001. Homologous and heterologous *Borrelia burgdorferi* challenge of infection-derived immune rabbits using host-adapted organisms. Infect. Immun. **69:** 593–598.
49. **Simpson, W. J., W. Cieplak, M. E. Schrumpf, A. G. Barbour, and T. G. Schwan.** 1994. Nucleotide sequence and analysis of the gene in *Borrelia burgdorferi* encoding the immunogenic P39 antigen. FEMS Microbiol. Lett. **119:**381–387.
50. **Simpson, W. J., M. E. Schrumpf, and T. G. Schwan.** 1990. Reactivity of human Lyme borreliosis sera with a 39-kilodalton antigen specific to *Borrelia burgdorferi*. J. Clin. Microbiol. **28:**1329–1337.
51. **Skare, J. T., T. A. Mirzabekov, E. S. Shang, D. R. Blanco, H. Erdjument-Bromage, J. Bunikis, S. Bergstrom, P. Tempst, B. L. Kagan, J. N. Miller, and M. A. Lovett.** 1997. The Oms66 (p66) protein is a *Borrelia burgdorferi* porin. Infect. Immun. **65:**3654–3661.
52. **Skare, J. T., E. S. Shang, D. M. Foley, D. R. Blanco, C. I. Champion, T. Mirzabekov, Y. Sokolov, B. L. Kagan, J. N. Miller, and M. A. Lovett.** 1995. Virulent strain associated outer membrane proteins of *Borrelia burgdorferi*. J. Clin. Investig. **96:**2380–2392.
53. **Suk, K., S. Das, W. Sun, B. Jwang, S. W. Barthold, R. A. Flavell, and E. Fikrig.** 1995. *Borrelia burgdorferi* genes selectively expressed in the infected host. Proc. Natl. Acad. Sci. USA **92:**4269–4273.
54. **Sung, S. Y., J. V. McDowell, J. A. Carlyon, and R. T. Marconi.** 2000. Mutation and recombination in the upstream homology box-flanked *ospE*-related genes of the Lyme disease spirochetes result in the development of new antigenic variants during infection. Infect. Immun. **68:**1319–1327.
55. **Wallich, R., C. Brenner, M. D. Kramer, and M. M. Simon.** 1995. Molecular cloning and immunological characterization of a novel linear-plasmid-encoded gene, pG, of *Borrelia burgdorferi* expressed only in vivo. Infect. Immun. **63:**3327–3335.
56. **Wallich, R., M. M. Simon, H. Hofmann, S. E. Moter, U. E. Schaible, and M. D. Kramer.** 1993. Molecular and immunological characterization of a novel polymorphic lipoprotein of *Borrelia burgdorferi*. Infect. Immun. **61:** 4158–4166.
57. **Yang, L., J. H. Weis, E. Eichwald, C. P. Kolbert, D. H. Persing, and J. J. Weis.** 1994. Heritable susceptibility to severe *Borrelia burgdorferi*-induced arthritis is dominant and is associated with persistence of large numbers of spirochetes in tissues. Infect. Immun. **62:**492–500.
58. **Zhang, J. R., J. M. Hardham, A. G. Barbour, and S. J. Norris.** 1997. Antigenic variation in Lyme disease borreliae by promiscuous recombination of VMP-like sequence cassettes. Cell **89:**275–285.
59. **Zhang, J. R., and S. J. Norris.** 1998. Genetic variation of the *Borrelia burgdorferi* gene *vlsE* involves cassette-specific, segmental gene conversion. Infect. Immun. **66:**3698–3704.
60. **Zhang, J. R., and S. J. Norris.** 1998. Kinetics and in vivo induction of genetic variation of *vlsE* in *Borrelia burgdorferi*. Infect. Immun. **66:**3689–3697.

Editor: D. L. Burns